Electronic Supplementary Information (ESI) for:

Identifying active site of ultrathin NiCo LDH as efficient peroxidase mimic with superior substrate affinity for sensitive detection of hydrogen peroxide

Yue Sun[a], Hai Xu[a], Xi Zhao[a], Zengyu Hui[a], Chenyang Yu[a], Lumin Wang[a], Jialu Xue[a], Yue Zhao[a], Ruicong Zhou[a], Henghan Dai[a], Chunyang Miao[a,*], Qiang Chen[c], Jinyuan Zhou[d], Gengzhi Sun[a,b,*], Wei Huang[a,b]

[a]Institute of Advanced Materials (IAM), Nanjing Tech University (NanjingTech), Nanjing 211816, P. R. China

[b]Institute of Flexible Electronics (IFE), Northwestern Polytechnical University, Xi'an 710072, P. R. China

[c]School of Materials Science and Engineering, Henan Polytechnic University, Jiaozuo, 454003, P. R. China

[d]School of Physical Science and Technology, Lanzhou University, Lanzhou 730000, P. R. China

*Corresponding author.

Email address: iamgzsun@njtech.edu.cn (Gengzhi Sun)

Contents:

1 Materials and methods

1.1. Materials and reagents

$Ni(NO_3)_2 \cdot 6H_2O$ (99.9%, AR grade), $Co(NO_3)_2 \cdot 6H_2O$ (99.9%, AR grade), NaOH (99.98%, AR grade), H_2O_2 (30%) were purchased from Shanghai Ling Feng Chemical Reagent Co., Ltd. TMB, glucose, sucrose, ascorbic acid (AA), dopamine (DA) and citric acid (CA) were obtained from Shanghai Energy Chemical Co., Ltd. Real milk samples were purchased from the supermarket in Nanjing (China). All other chemicals were used directly without further purification.

1.2. Characterizations

Kinetic measurements and UV-Vis absorption spectra were carried out on UV-1600 (Shanghai Mapada Instrument Co., Ltd, China). Transmission electron microscopy (JEOL JEM-1400F) and X-ray diffraction (Rigaku-Ultima III XRD, Cu K_α radiation, λ= 1.5418 Å) were performed to characterize the morphology and crystal structure of NiCo LDHs. Fourier transform infrared spectroscopy (KBr as pellets, Thermo Nicolet-380 IR spectrophotometer (USA)) was utilized to investigate the surface properties of NiCo LDHs. Raman spectra were recorded on a WITeck CRM200 confocal Raman system with a laser of 633 nm. X-ray photoelectron spectroscopy (XPS) spectra were recorded on a PHI Quantera spectrometer.

1.3. Synthesis of NiCo LDH

NiCo LDH nanosheets were prepared by a fast co-precipitation at room temperature developed in our previous studies. Briefly, a mixed solution containing 1.5 mmol of $Ni(NO_3)_2$ and $Co(NO_3)_2$ were quickly added into 20 ml of NaOH aqueous solution (0.15 M) under vigorous stirring. The ratio between $Ni(NO_3)_2$ and $Co(NO_3)_2$ was adjusted to tune the final composition in NiCo LDH. Once the collected green precipitation underwent repetitive washing and mild ultrasonication for three times, the obtained NiCo LDH nanosheets were stably and homogeneously re-dispersed in deionized (DI) water with a concentration of 1 mg ml^{-1}.

1.4. The catalytic activity of NiCo LDH nanozyme

The catalytic activity was evaluated by using H_2O_2 and TMB as the substrates. Typically, the feasibility of NiCo LDHs for H_2O_2 detection was performed in 1 ml PBS solution (10 mM, PH=5.39) containing 166 μM TMB, and the amount of NiCo LDHs was fixed at 10 μg. The apparent kinetic parameters were calculated based on the Michaelis-Menten equation of $\upsilon = V_{max} \times [S] / (K_m + [S])$, where K_m is Michaelis-Menten constant implying the affinity

between substrate and enzyme, and υ, V_{max} and [S] is the initial velocity, the maximal reaction velocity and the substrate concentration, respectively.

1.5. Colorimetric detection of H_2O_2 in milk sample

4 ml raw milk was firstly diluted to 10 ml with water. Then the milk was centrifuged at 12500 rpm for 60 min to remove the protein, fat and other organic substances and separate the deposit. Thirdly, the supernatant was centrifuged at 11000 rpm for 30 min to remove the deposit once again. The final solution was collected and mixed with TMB-H_2O_2 reaction system.

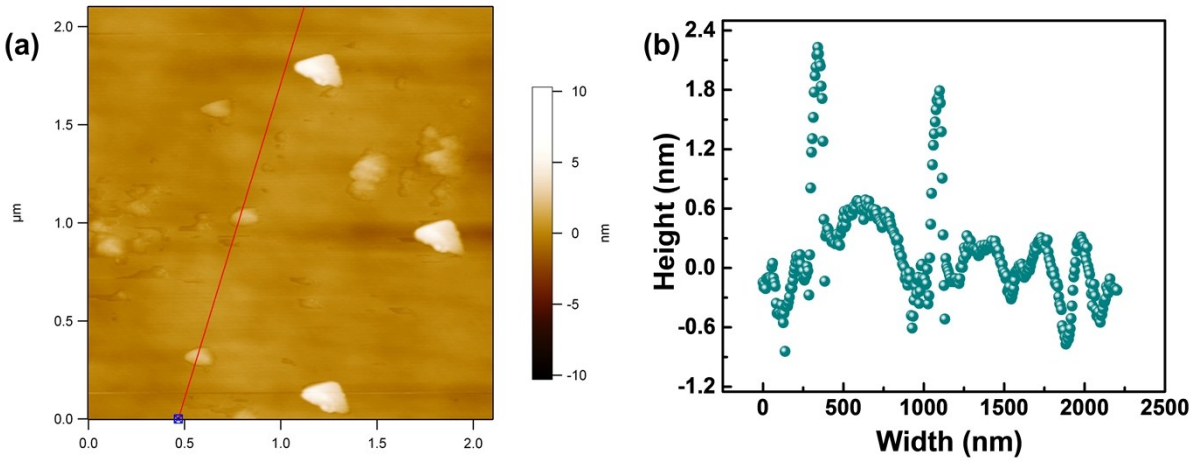

Figure S1. (a) AFM image of ultrathin $Ni_{0.67}Co_{0.33}$ LDH. (b) Height profile of ultrathin $Ni_{0.67}Co_{0.33}$ LDH at the red dash line in panel (a).

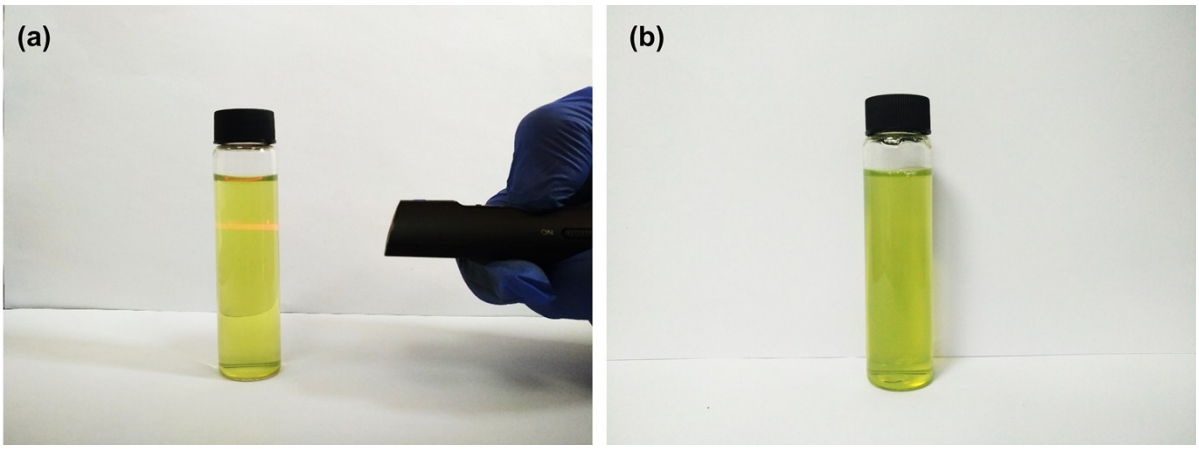

Figure S2. (a) Photo iamge of $Ni_{0.67}Co_{0.33}$ LDH dispersion with Tyndall effect. (b) Photo image of $Ni_{0.67}Co_{0.33}$ LDH dispersion kept at room temperature for one month.

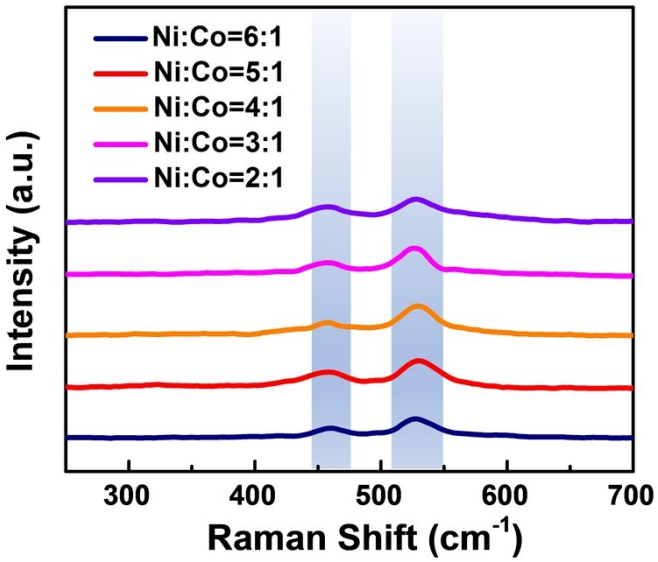

Figure S3. Raman spectra of the NiCo LDHs with different Ni:Co molar ratios.

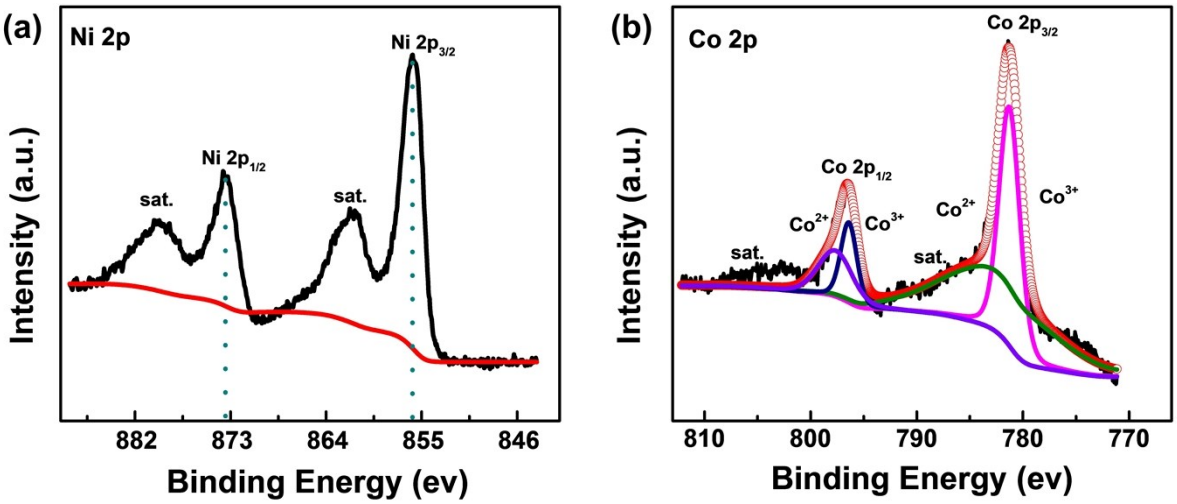

Figure S4. XPS spectra of (a) Ni 2p and (b) Co 2p for $Ni_{0.67}Co_{0.33}$ LDH nanosheets.

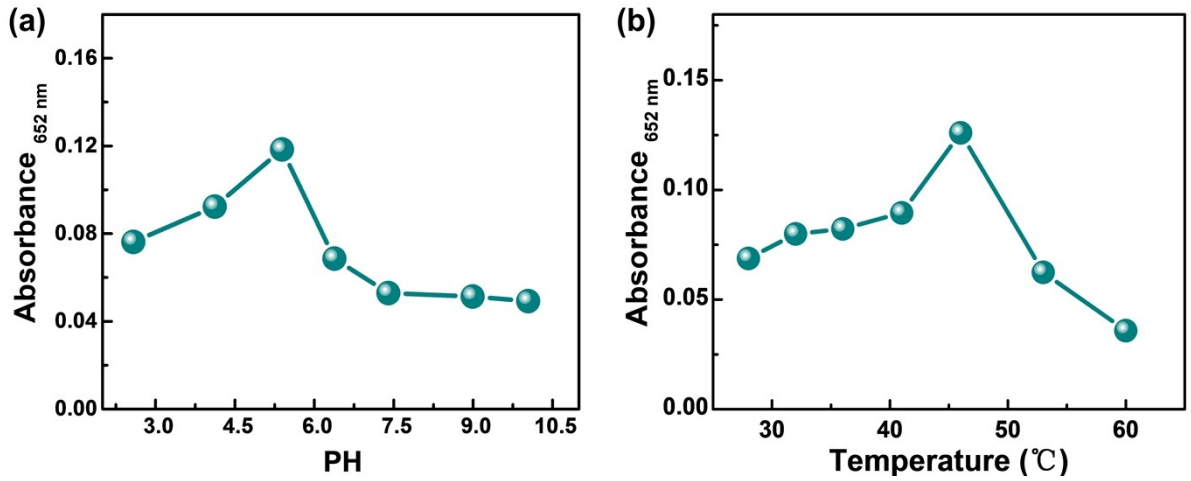

Figure S5. (a) pH and (b) temperature dependent peroxidase-like activity of $Ni_{0.67}Co_{0.33}$ LDH. The experiments were carried out using 10 μL of 1 mg ml^{-1} $Ni_{0.67}Co_{0.33}$ LDHs in 1 mL of 10 mM PBS with 314 μM H_2O_2 and 166 μM TMB as substrates.

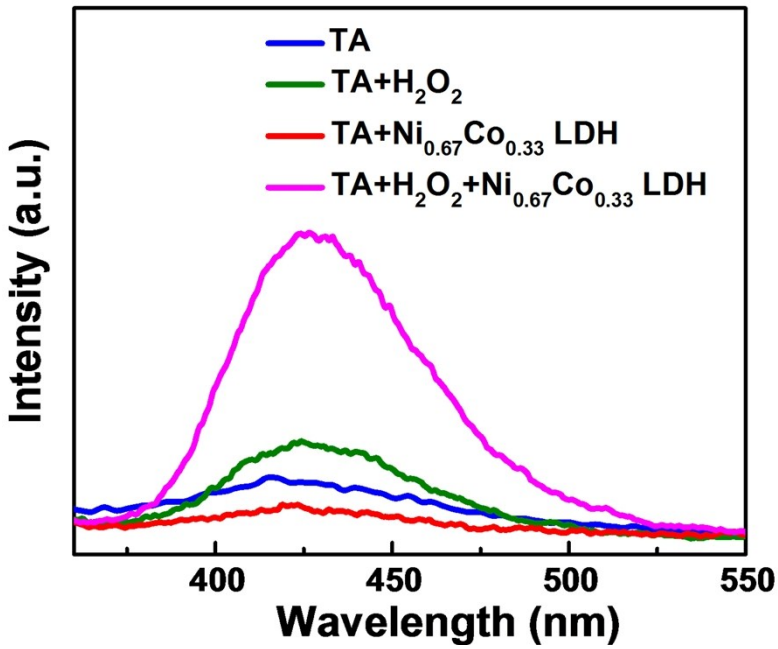

Figure S6. The fluorescence spectra of TA (blue line), TA+H_2O_2 (green line), TA+$Ni_{0.67}Co_{0.33}$ LDH (red line) and TA+H_2O_2+$Ni_{0.67}Co_{0.33}$ LDH (purple line), respectively. The fluorescence spectrum was recorded ranging from 350 to 550 nm with the excitation wavelength of 315 nm.

Table S1. Performance comparison of K_m of different nanozymes.

Catalyst	K_m (mM)		References[1-13]
	TMB	H_2O_2	
HRP	0.434	3.7	1
V_2O_5	0.738	0.232	2
Fe_3O_4	0.098	154	1
NiO	6.66	208	3
6Fe/CeO_2	0.176	47.6	4
Fe_2O_3 nanocubes	0.214	115	5
CeO_2	0.274	0.278	6
$ZnFe_2O_4$ MNPs	0.85	1.66	7
Co_3O_4	0.103	173.51	8
CoAl LDH	0.372	22.13	9
NiFe LDH	2.4	0.5	10
DNA/CuAl LDH	1.775	10.24	11
C-dot/NiAl LDH	0.34	4.72	12
CoOOH	2.02	0.06	13
This work	0.0478	0.061	-

Table S2. Performance comparison with other H_2O_2 sensors.

nanomaterials	Linear range (mM)	Detection limit (μM)	References[14-20]
NiFe-LDH	0.01-0.5	4.4	11
DNA/CuAl-LDH	0.02-3	10	12
CoAl LDH	0.01-0.02	10	10
Co_3O_4 NPs	0.01-4	10	14
Pt-DNA complexes	0.979-17.6	392	15
BSA-templated Pt-NPs	0.05-3	7.9	16
Ni-Bi/CC	0.0001-0.5	0.00085	17
Co_3N NW/CF	0.002-28	1	18
Cu_3N NW/CF	0.0001-10	0.0089	19
Ni_2P NA/TM	0.001-20	0.2	20
This work	0.01-1.256	0.48	-

2. References

1. L. Gao, J. Zhuang, L. Nie, J. Zhang, Y. Zhang, N. Gu, T. Wang, J. Feng, D. Yang, S. Perrett and X. Yan, *Nat. Nanotechnol.*, 2007, **2**, 577-583.
2. Y. Wang, J. Liu, J. Jiang and W. Zhong, *Anal. Bioanal. Chem.*, 2017, **409**, 4225-4232.
3. Q. Liu, Y. Yang, H. Li, R. Zhu, Q. Shao, S. Yang and J. Xu, *Biosens. Bioelectron.*, 2015, **64**, 147-153.
4. D. Jampaiah, T. Srinivasa Reddy, A.E. Kandjani, P.R. Selvakannan, Y.M. Sabri, V.E. Coyle, R. Shukla and S.K. Bhargava, *J. Mater. Chem. B*, 2016, **4**, 3874-3885.
5. M. Zhu, Y. Dai, Y. Wu, K. Liu, X. Qi and Y. Sun, *Nanotechnology*, 2018, **29**, 465704.
6. Q. Liu, Y. Yang, X. Lv, Y. Ding, Y. Zhang, J. Jing and C. Xu, *Sensor Actuat. B-Chem.*, 2017, **240**, 726-734.
7. L. Su, J. Feng, X. Zhou, C. Ren, H. Li and X. *Chen, Anal. Chem.*, 2012, **84**, 5753-5758.
8. J. Dong, L. Song, J. Yin, W. He, Y. Wu, N. Gu and Y. Zhang, *ACS Appl. Mater. Interfaces*, 2014, **6**, 1959-1970.
9. L. Chen, B. Sun, X. Wang, F. Qiao and S. Ai, *J. Mater. Chem. B*, 2013, **1**, 2268.
10. T. Zhan, J. Kang, X. Li, L. Pan, G. Li and W. Hou, *Sensor Actuat. B-Chem.*, 2018, **255**, 2635-2642.
11. L. Chen, K. Sun, P. Li, X. Fan, J. Sun and S. Ai, *Nanoscale*, 2013, **5**, 10982.
12. Y. Guo, X. Liu, X. Wang, A. Iqbal, C. Yang, W. Liu and W. Qin, *RSC Adv.*, 2015, **5**, 95495-95503.
13. J. Sun, C. Li, Y. Qi, S. Guo and X. Liang, *Sensors*, 2016, **16**, 584.
14. J. Mu, L. Zhang, M. Zhao and Y. Wang, *J. Mol. Catal. A Chem.*, 2013, **378**, 30-37.
15. F. Xu, Y. Sun, Y. Zhang, Y. Shi, Z. Wen and Z. Li, *Electrochem. Commun.*, 2011, **13**, 1131-1134.
16. L. Chen, N. Wang, X. Wang and S. Ai, *Microchim. Acta*, 2013, **180**, 1517-1522.
17. Z. Wang, F. Xie, Z. Liu, G. Du, A. M. Asiri and X. Sun, *Chem. Eur. J.*, 2017, **23**, 16179-16183.
18. F. Xie, X. Cao, F. Qu, A. M. Asiri and X. Sun, *Sensor Actuat. B-Chem.*, 2018, **255**, 1254-1261.
19. Z. Wang, X. Cao, D. Liu, S. Hao, R. Kong, G. Du, A. M. Asiri and X. Sun, *Chem. Eur. J.*,

2017, **23**, 4986-4989.

20. X. Xiong, C. You, X. Cao, L. Pang, R. Kong and X. Sun, *Electrochim. Acta*, 2017, **253**, 517-521.